https://doi.org/10.15407/ujpe69.6.373

P.S. DANYLYUK,[1] G.V. RIZAK,[1] O.I. GOMONAI,[2] P.P. PUGA,[1] A.O. FROLOV,[1] A.N. GOMONAI,[2] V.M. RIZAK [1]

[1] Uzhhorod National University
(54, Voloshyna Str., Uzhgorod 88000, Ukraine)
[2] Institute of Electron Physics, Nat. Acad. of Sci. of Ukraine
(21, Universytets'ka Str., Uzhgorod 88017, Ukraine)

RAMAN SCATTERING IN GLASSY LITHIUM TETRABORATE ACTIVATED WITH ERBIUM AND TERBIUM OXIDES

Spectra of Raman scattering in glassy lithium tetraborate activated with erbium and terbium oxides to various concentrations have been studied. It is found that the main components of the observed structures in the Raman scattering spectra of $Li_2B_4O_7 : Er_2O_3$ and $Li_2B_4O_7 : Tb_2O_3$ glasses obtained in the framework of a medium-order approximation are induced by mixed vibrations of complicated boron/lithium/erbium/terbium-oxygen structural complexes.

K e y w o r d s: Raman scattering, lithium tetraborate, erbium oxide, terbium oxide, structural complexes, mixed vibrations, phonons.

1. Introduction

Compounds based on lithium tetraborate ($Li_2B_4O_7$, LTB) are widely used in various fields of science and technology due to their high radiation resistance, transparency in a wide spectral interval, high values of nonlinear optical coefficients, and so forth [1–5]. In particular, they are applied as nonlinear elements for generating harmonics and total frequencies of laser radiation, as well as a material for tissue-equivalent thermoluminescent radiation detectors. Doping an LTB matrix with ions of rare earth elements substantially improves its luminescent properties, which allows such compounds to be used as efficient phosphors, fiber lasers and amplifiers, optical memory devices, three-dimensional displays, and others. LTB is also applied as a superionic conductor (solid electrolyte) for solid-state sources of electricity. For such electrolytes, important is information on the relation between their structure and ionic conductivity, which depends on the nature of the interaction of superionic complexes in the B_2O_3–Li_2O system. Convenient tools for studying their structure are Raman and IR spectroscopies.

As is known, the structure of crystalline LTB is described by the space group $I4_1cd(C_{4v}^{12})$ [6, 7]. A unit cell of tetragonal symmetry ($a = b = 9.479$ Å, $c = 10.286$ Å) contains 8 formula units of $Li_2B_4O_7$ (104 atoms). Bulk boron-oxygen complexes $[B_4O_9]^{6-}$ consist of two planar triangles $[BO_3]$ and two tetrahedra $[BO_4]$ with a strong covalent bond [8], which are united by oxygen atoms common to neighboring complexes into a spiral with the axis parallel to the **c**-axis; by means of common oxygen atoms, those structures create a three-dimensional rigid frame-

C i t a t i o n: Danylyuk P.S., Rizak G.V., Gomonai O.I., Puga P.P., Frolov A.O., Gomonai A.N., Rizak V.M. Raman scattering in glassy litium tetraborate activated with erbium and terbium oxides. *Ukr. J. Phys.* **69**, No. 6, 373 (2024). https://doi.org/10.15407/ujpe69.6.373.

Цитування: Данилюк П.С., Різак Г.В., Гомонай О.І., Пуга П.П., Фролов А.О., Гомонай Г.М., Різак В.М. Комбінаційне розсіювання світла склоподібним тетраборатом літію, активованим оксидами ербію та тербію. *Укр. фіз. журн.* **69**, №6, 373 (2024).

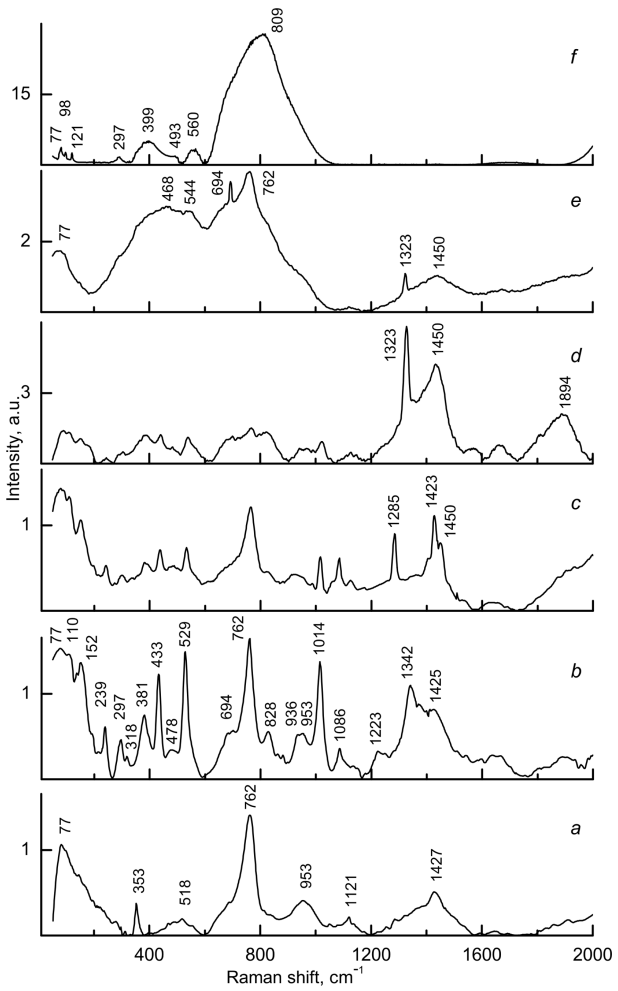

Fig. 1. Raman spectra of glassy $Li_2B_4O_7$ activated with $Er_2O_3$to 0.000 (*a*), 0.0005 (*b*), 0.001 (*c*), 0.005 (*d*), 0.01 (*e*), and 0.05 wt% (*f*)

work. Lithium cations are located in the channels of this framework along the direction parallel to the optical crystal axis. The first coordination sphere of the lithium atom includes the four nearest oxygen atoms, which create a highly deformed tetrahedron. The chains of lithium-oxygen tetrahedra are wound on the 4_1-axis.

Taking into account that, in the framework of the medium order approximation [9], single crystals and glasses of lithium tetraborate are practically isostructural, we may assume that glassy $Li_2B_4O_7$ has a similar structure, but with slightly deformed unit cell parameters, which makes some corrections to the dynamics of the deformed LTB structure.

It is known that the spectra of Raman scattering (RS) in glassy materials contain information about the short-range structure [10]. Correlations with the spectra of crystals possessing similar structures (in the framework of the short-range order that includes several coordination spheres) often manifest themselves. In addition, RS in glasses is stronger than the ordinary second-order RS in crystals [11, 12]. Raman spectra of glasses can contain relatively narrow bands typical of first-order scattering in crystals. Since glass disordering leads to the cancellation of selection rules at $\mathbf{k} = 0$ [12], all vibrational modes can contribute to the scattering nature [11]. This circumstance testifies that RS in glasses is a first-order scattering and is closely related to the density of vibrational states.

The study of Raman spectra of glassy $Li_2B_4O_7$ doped with rare earth elements has not received due attention in the literature, and the relevant data are extremely limited today. The aim of this work was to experimentally study the RS effects in doped glassy lithium tetraborate activated with erbium and terbium ions, which enter the structure of the LTB matrix in the form of triply charged Er^{3+} and Tb^{3+} ions. Note that unlike other rare earth oxides, Tb_2O_3 forms compounds with mixed valence and a stoichiometric matrix structure [13–15].

2. Experimental Part

Raman spectra were studied on a micro Raman spectrometer XploRA PLUS (HORIBA Jobin Yvon). The spectra were excited by means of laser radiation with a wavelength of 785 nm. The research was carried out at a temperature of 300 K in the spectral interval 70–2000 cm^{-1} with a resolution not worse than 1 cm^{-1}.

Glassy $Li_2B_4O_7$ specimens used in this work were synthesized following the technology described in work [16]. Their activation with erbium and terbium oxides was carried out to the following weight percentages: 0.0005, 0.001, 0.005, 0.01, and 0.05 wt%.

3. Results and Their Discussion

The results of research on the Raman spectra of glassy LTB specimens activated with erbium and terbium oxides to various concentrations (0.0005–0.05 wt%) are shown in Figs. 1, *b*–*f* and Figs. 2, *b*–*f*, respectively. For comparison, panels *a* in both figures demonstrate the Raman spectrum of stoichiometric $Li_2B_4O_7$. Note that the positions of seven distinct

Raman bands observed at the frequencies 77, 353, 518, 762, 953, 1121, and 1427 cm^{-1} in this case are in good agreement with literature data obtained by other authors in the limited spectral interval 300–1500 cm^{-1} [9, 17–21].

As for the nature of vibrational modes in glassy stoichiometric $Li_2B_4O_7$, it was considered in detail by us in work [22]. Here, we only recall that the wide asymmetric maximum at the frequency 77 cm^{-1}, which consists of several closely spaced unresolved bands, is mainly associated with normal vibrations of the $[LiO_6]$ frameworks. The maxima at the frequencies 353 and 518 cm^{-1} are associated with the superposition of vibrations of the framework groups $[LiO_4]$ and the tetrahedra $[BO_4]$. The most intensive maximum in the spectrum at the frequency 762 cm^{-1} is a result of oscillating symmetric deformations of the $[BO_3]$ complexes. The broad maximum at the frequency 953 cm^{-1} is associated with the deformation of $[BO_4]$ tetrahedra and the symmetric stretching of the $[BO_3]$ group. The low-intensity maximum at the frequency 1121 cm^{-1} is caused by vibrations inherent to distorted tetrahedra [23]. Finally, the broad maximum at the frequency 1427 cm^{-1} is associated with the symmetric stretching of planar triangles $[BO_3]$ and vibrations of various borate rings.

3.1. Raman spectra of glassy $Li_2B_4O_7 : Er_2O_3$

At the activation of $Li_2B_4O_7$ with the Er_2O_3 impurity to 0.0005 wt%, the structure of the Raman spectrum becomes much more complicated, which manifests itself in an increase of the number of observed features (Fig. 1, *b*). In particular, in the spectral interval 70–600 cm^{-1}, 10 intensive bands are observed at the frequencies 77, 110, 152, 239, 297, 318, 381, 433, 478, and 529 cm^{-1}. In the frequency interval 600–860 cm^{-1}, an intensive band at the frequency 762 cm^{-1} and with clearly pronounced features at the frequencies 694 and 828 cm^{-1} was registered; this band is also characteristic of stoichiometric glassy LTB (Fig. 1, *a*).

For the $Li_2B_4O_7 : 0.0005$ wt% Er_2O_3 compound, a group of closely spaced lines at the frequencies 936, 953, and 1014 cm^{-1} can be observed in the spectral interval 860–1050 cm^{-1}, in contrast to the stoichiometric composition (Fig. 1, *a*), which demonstrates a broad band with a maximum at 953 cm^{-1} in this

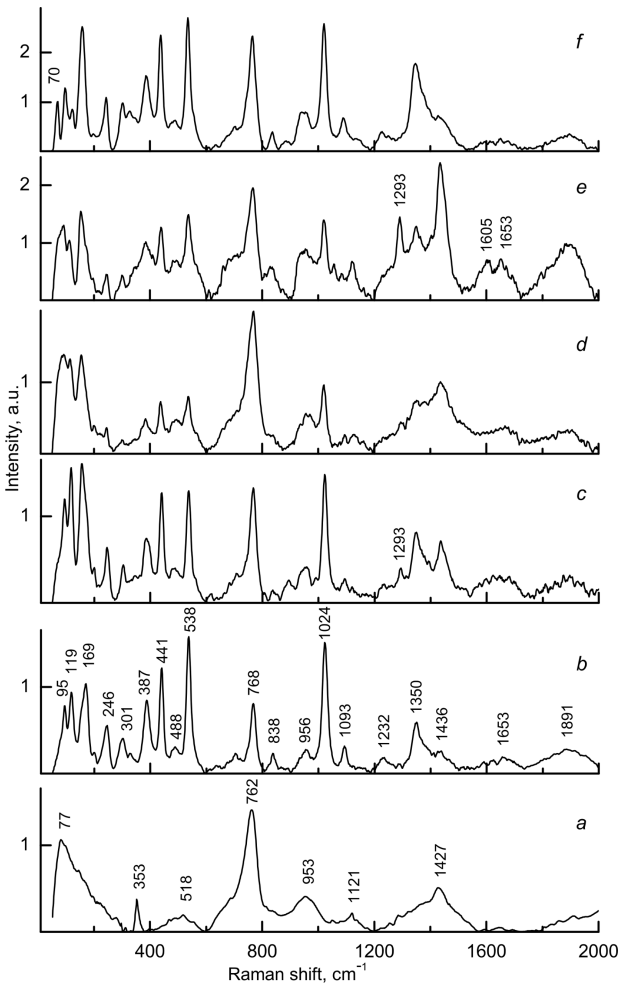

Fig. 2. Raman spectra of glassy $Li_2B_4O_7$ activated with Tb_2O_3 to 0.000 (*a*), 0.0005 (*b*), 0.001 (*c*), 0.005 (*d*), 0.01 (*e*), and 0.05 wt% (*f*)

interval. In the spectral interval 1050–2000 cm^{-1}, after the LTB activation with Er_2O_3, additional vibrational bands appear at the frequencies 1086, 1223, 1342, and 1425 cm^{-1} against the background of the Raman spectrum of glassy $Li_2B_4O_7$ (a broad diffuse band at the frequency 1427 cm^{-1}).

When 0.001 wt% of Er_2O_3 is introduced into the LTB matrix (Fig. 1, *c*), the structure of the Raman spectrum (the intensities and the frequency positions of the vibrational bands) does not change substantially, except for the interval 1200–1500 cm^{-1} where narrow lines at the frequencies 1285, 1423, and 1450 cm^{-1} are clearly observed against a broad-band background.

As the Er_2O_3 concentration increases to 0.005 wt% (Fig. 1, *d*), the intensities of the Raman bands in the spectral interval 1200–2000 cm^{-1} grow substantially, but their positions practically do not change (Fig. 1, *b–d*). Additionally, the broadening of the Raman bands is observed within the whole examined spectral interval, and a distinct diffuse vibrational band appears at the frequency 1894 cm^{-1}.

As the activator concentration increases further to 0.01 wt% (Fig. 1, *e*), an essential transformation of the Raman spectrum takes place. In particular, a redistribution of the Raman intensity is observed in a frequency interval of 200–1600 cm^{-1} and a considerable expansion of the vibrational bands in the whole frequency interval. In this case, seven bands are observed in the Raman spectrum at the frequencies 77, 468, 544, 694, 762, 1323, and 1450 cm^{-1}, with weakly pronounced features at 297, 380, 828, and 953 cm^{-1}.

At the activator concentration 0.05 wt% Er_2O_3 (Fig. 1, *f*), vibrational modes are observed in the Raman spectrum at the frequencies 77, 98, 121, 297, 399, 493, and 560 cm^{-1}, and an intensive broad asymmetric band within the interval 600–1100 cm^{-1}, with a maximum at the frequency 809 cm^{-1}, and weakly pronounced features at the frequencies 694, 762, and 828 cm^{-1}.

Note that a comparison of our Raman spectra obtained at the Er_2O_3 concentrations 0.0005–0.005 wt% with the Raman spectrum of single-crystalline LTB measured in unpolarized light [19] testifies to an almost complete coincidence of the frequencies of vibrational modes within the spectral interval 80–2000 cm^{-1}. This circumstance allows us to assume that when glassy $Li_2B_4O_7$ is activated with Eg^{3+} ions, clustering processes occur in the disordered matrix up to the concentration 0.005 wt% inclusive, at which the structure of glassy LTB may remain tetragonal in the framework of the medium-range order. This assumption is consistent with the results of work [24].

Let us now consider the origin of the vibrational structure for glassy $Li_2B_4O_7 : Er_2O_3$. For the Er_2O_3 concentrations 0.0005–0.005 wt%, the Raman spectra consist of separate groups of closely located lines (Fig. 1, *b–d*). The most intensive lines are observed in the spectral intervals 70–200, 700–800, and 1300–1500 cm^{-1}. In this case, according to works [25–30], fundamental vibrations appear in the frequency interval 77–1500 cm^{-1}. The absence of vibrations with lower frequencies testifies to the growth of the glassy matrix stiffness and reflects the specific features of the deformed framework structure of $Li_2B_4O_7$ glass. This is also confirmed by a certain difference between the frequency positions of normal vibrations and the modes in the Raman spectrum of crystalline LTB.

In our opinion, the broad structural diffuse band with maxima at 1342 and 1425 cm^{-1}, which is observed in the frequency interval 1300–1500 cm^{-1}, is a manifestation of two-phonon states ($\nu = 1425$ cm^{-1}). The most probable here is the availability of overtones and components of vibrational tones in the frequency interval 694–780 cm^{-1}. The maximum at the frequency 1342 cm^{-1} characterizes the vibrations of borate rings and the symmetrical stretching of flat BO_3 triangles. The diffuse maxima at the frequencies 1648 and 1894 cm^{-1} are responsible for normal vibrations of boron-oxygen, B–O, bonds [20, 31]. According to the data of works [9, 29, 32, 33], the interval 900–1050 cm^{-1} corresponds to the symmetric stretching of the BO_3 group (at 936, 953, and 1014 cm^{-1}), whereas the interval 600–900 cm^{-1} corresponds to the asymmetric deformation of flat BO_3 triangles (at 694 cm^{-1}) and the vibrations of oxygen bridges between a tetrahedral boron atom and a trigonal one, as well as between a tetrahedral boron atom and two trigonal ones.

Note that, in this frequency interval, vibrations responsible for the distorted modes of BO_4 groups are also observed. The intensive maximum at the frequency 762 cm^{-1} characterizes the symmetrical deformation of flat BO_3 triangles. The interval 400–600 cm^{-1} corresponds to mixed translational (at 433 and 478 cm^{-1}) and ordinary (at 528 cm^{-1}) vibrations of lithium ions. In addition, the spectra of lithium borates with tetrahedral groups $[LiO_4]$ contain characteristic lines in the frequency interval 200–400 cm^{-1}, which correspond to the vibrational modes of the $[LiO_6]$ frameworks. The vibrations in this spectral interval (200–300 cm^{-1}) can also be attributed to the vibrations of the BO_3 and BO_4 groups in the structure of the $[B_4O_7]^{2-}$ cluster as a whole, which leads to the deformation of the latter [34].

The spectral interval 0–200 cm^{-1} (the lines at 71, 110, and 152 cm^{-1}) characterizes the "external" modes of structural complexes that are included in the matrix of glassy $Li_2B_4O_7$. In addition, normal vibrations of ligands with Eg^{3+} ions in LTB struc-

tural complexes can also contribute to this interval (Fig. 1, *b*–*d*) [31].

At an Er_2O_3 concentration of 0.01 wt% (Fig. 1, *e*), the vibrational modes at the frequencies 1323, 1329, and 1450 cm^{-1}, which correspond to vibrations of the $[LiO_4]$ clusters, partially survive in the Raman spectrum. In the interval 400–600 cm^{-1}, according to work [28], a superposition of vibrations of $[LiO_4]$ groups and $[BO_4]$ tetrahedra takes place. The bands at the frequencies 694 and 762 cm^{-1}, as it occurs in the case of other spectra (Fig. 1, *a*–*d*), are responsible for the vibrations of oxygen bridges between a tetrahedral boron atom and a trigonal one, and between a tetrahedral boron atom and two trigonal ones, as well as for the symmetric deformation of planar triangles of $[BO_3]$ groups, respectively.

In the case of the maximum studied impurity concentration (0.05 wt% Er_2O_3) (Fig. 1, *f*), the Raman spectrum demonstrates quite clearly the maxima that according to their energy positions (at 77, 98, 121, 297, 399, 493, and 560 cm^{-1}) correspond to the Raman spectrum of Er_2O_3 oxide with cubic system within the spectral interval 70–600 cm^{-1} and agree well with the data of works [34–39]. Two groups of vibrations can be distinguished in this frequency interval of optically active phonons. Internal vibrations owing to the distortion of octahedral $[Er_2O_6]$ clusters prevail in one group (above 300 cm^{-1}), and translational vibrations of octahedra and Eg^{3+} ions (Eg^{3+}–O–Eg^{3+} or O–Eg^{3+}–O) in the glassy structure of Eg^{3+}–$Li_2B_4O_7$ dominate in the other group (below 200 cm^{-1}).

These results agree with the data of work [24] The cited authors, on the basis of EXAFS (extended X-ray absorption fine structure) spectra and theoretical calculations, showed that, when glassy LTB is activated, the hybridization of triply charged ions of rare earth elements (in our case, Eg^{3+}) with the LTB matrix takes place. Since B_4O_7 borates in the $Li_2B_4O_7$ matrix are connected by strong covalent bonds, the Er^{3+} ions most likely occupy the positions of Li^+ ions (the latter are connected with basic borates via ionic bonds [40]) and form structural complexes [Er^{3+}–$Li_2B_4O_7$] through the bonds with oxygen atoms with coordination numbers within an interval of 6–8. It should be noted that erbium atoms are much heavier than oxygen ones; therefore, the motion of oxygen atoms plays a dominant role in the vibrational stretching modes of Er–O bonds [41].

The broad diffuse maximum observed in the frequency interval 600–1000 cm^{-1} (Fig. 1, *f*), as it is in the other spectra, arises due to the asymmetric deformation of flat BO_3 triangles (the feature at 694 cm^{-1}) and the superposition of vibrations of oxygen bridges between tetragonal and trigonal boron atoms. In addition, the superposition of indicated vibrations and the vibrations of octahedral $[ErO_6]$ complexes can also contribute to this band.

3.2. Raman spectra of glassy $Li_2B_4O_7 : Tb_2O_3$

In the researched Raman spectra of glassy $Li_2B_4O_7 : Tb_2O_3$, four intervals can be conditionally distinguished. They correspond to the main groups of observed maxima within intervals of 70–600, 600–850, 850–1200, and 1200–2000 cm^{-1}.

When activating $Li_2B_4O_7$ with the Tb_2O_3 admixture to 0.0005–0.05 wt%, the structure of the Raman spectra becomes substantially complicated in comparison with that for the stoichiometric composition (Fig. 2, *b*–*f*). For instance, in the spectral interval 70–600 cm^{-1}, instead of three bands (Fig. 2, *a*), eight intensive vibrational bands are observed at the frequencies 95, 119, 169, 246, 301, 387, 441, and 538 cm^{-1}, as well as a low-intensity band at the frequency 488 cm^{-1}. The positions of those bands practically do not change as the Tb_2O_3 concentration grows. The only exception is the band observed at the frequency 169 cm^{-1} when the Tb_2O_3 concentration equals 0.0005 wt% (Fig. 2, *b*). With the further increase of the impurity concentration (Fig. 1, *c*–*f*), this band shifts towards lower frequencies (to 153 cm^{-1}). At the same time, if the Tb_2O_3 concentration grows further from 0.001 to 0.05 wt%, the position of this band does not change. At the maximum Tb_2O_3 concentration of 0.05 wt%, there appears a band in the Raman spectrum at the frequency 70 cm^{-1} (Fig. 2, *e*), which was absent at lower activator concentrations (Fig. 2, *b*–*e*). As the concentration of Tb_2O_3 grows, changes in the intensity ratios of the vibrational bands are observed in the considered spectral interval (70–600 cm^{-1}). Additionally, a clear broadening of those bands is observed for the compositions $Li_2B_4O_7 : 0.005$ wt% Tb_2O_3 and $Li_2B_4O_7 : 0.01$ wt% Tb_2O_3 (Fig. 2, *d*, *e*).

In the spectral interval 600–850 cm^{-1}, instead of the broad band with a maximum at the frequency 762 cm^{-1} (Fig. 2, *a*), a narrower band with a max-

imum at the frequency 768 cm^{-1} is observed irrespective of the activator concentration (0.0005–0.05 wt.%). The intensity of this band increases with the increasing impurity concentration (Figs. 2, *b*–*e*). In addition, in the considered spectral interval, there is also a low-intensity band at the frequency 838 cm^{-1}, which appears in the Raman spectra in the form of a rather clear maximum at all activator concentrations, except for 0.005 wt% Tb_2O_3 (Fig. 2, *d*).

In the frequency interval 850–1200 cm^{-1}, instead of two bands located at the frequencies 956 and 1121 cm^{-1} in the case of stoichiometric composition (Fig. 2, *a*), an intensive band with a maximum at the frequency 1024 cm^{-1} and a low-intensity band at the frequency 956 cm^{-1} are observed at all activator concentrations (Figs. 2, *b*–*f*). In addition, a band with a maximum at the frequency 1093 cm^{-1} is observed in the Raman spectra at the activator concentrations 0.0005, 0.001, and 0.05 wt% Tb_2O_3 (Figs. 2, *b*, *c*, *f*), and a band at the frequency 1121 cm^{-1} at the Tb_2O_3 concentration 0.01 wt% (Fig. 1, *e*). In the indicated frequency interval, the intensity ratios between the Raman bands also change with the increase of the activator concentration. The minimum intensity of the bands in this spectral interval is observed for the Tb_2O_3 concentrations 0.005 and 0.01 wt%.

In the frequency interval 1200–2000 cm^{-1}, instead of the broad peak located at the frequency 1427 cm^{-1} in the case of stoichiometric LTB (Fig. 2, *a*), a number of bands (at 1232, 1293, 1350, and 1436 cm^{-1}) are observed in the Raman spectra of activated specimens; their clear manifestation changes as the Tb_2O_3 concentration increases (Figs. 2, *b*–*f*). Furthermore, their intensity ratios also change. In particular, with the increase of the activator concentration, the intensity of the band with a maximum at the frequency 1350 cm^{-1} becomes lower than the intensity of the neighboring band with a maximum at the frequency 1436 cm^{-1}, which reaches its maximum at the Tb_2O_3 concentration 0.01 wt% (Fig. 2, *e*). At the same concentration, a band with a maximum at the frequency 1293 cm^{-1} distinctly manifests itself in the Raman spectrum; at other activator concentrations, it reveals itself very weakly (Figs. 2, *b*–*d*, *f*). At the maximum examined concentration of 0.05 wt.% Tb_2O_3, the intensity of the band with a maximum at the frequency 1350 cm^{-1} increases again, whereas the neighboring band (at 1436 cm^{-1}) is only weakly visible against its background (Fig. 2, *e*). As for the band at the frequency 1232 cm^{-1}, it appears rather clearly in the Raman spectra of activated LTB only at the impurity concentrations 0.0005 wt% Tb_2O_3 and 0.05 wt% Tb_2O_3 (Figs. 2, *b*, *f*). Note also that in this spectral interval, diffuse vibrational bands with maxima at the frequencies 1653 and 1891 cm^{-1} are observed in the Raman spectra of activated LTB. The intensities of those bands increase with the growing activator concentration and reach the maximum values at the Tb_2O_3 concentration 0.01 wt% (Fig. 2, *e*). With further increase of the Tb_2O_3 concentration decreases the intensity of those bands substantially (Fig. 2, *f*). On the other hand, at the concentration 0.01 wt% Tb_2O_3 (Fig. 2, *e*), two bands with maxima at the frequencies 1605 and 1653 cm^{-1} are observed instead of one band with a maximum at the frequency 1653 cm^{-1}.

Let us now consider the origin of the vibrational structure of glassy $Li_2B_4O_7 : Tb_2O_3$. When interpreting the observed Raman maxima, we based our analysis on the known vibrational frequencies of the structural complexes $[LiO_4]$, $[LiO_3]$, $[BO_4]$, and $[BO_3]$ in various compounds on the basis of $Li_2B_4O_7$ [9, 18–20, 28, 29, 32–34], as well as on the infrared and Raman spectra of Tb_2O_3 and Tb_4O_7 single crystals [13–15, 34, 39].

A comparison of our spectra with the Raman spectra of single-crystalline Tb_2O_3 with cubic system in a frequency interval of 70–600 cm^{-1} [15] demonstrates a good (if we take into account the inclusion of Tb_2O_3 into the disordered LTB matrix) coincidence of the frequencies of the maxima at 95, 119, 169 (153), 301, 387, 441, and 538 cm^{-1}, which are observed in both spectra. The indicated frequencies correspond to one-, two-, and three-dimensional symmetric vibrations of the structural complexes included in the matrix of $Li_2B_4O_7 : Tb_2O_3$. In the considered frequency interval (70–600 cm^{-1}), two groups of optically active vibrations can be distinguished. In our opinion, internal vibrations associated with distortions of octahedral $[Tb_2O_7]$ clusters prevail in the first group (>200 cm^{-1}), whereas translational vibrations of these octahedra and Tb^{3+} ions (Tb^{3+}–O–Tb^{3+} or O–Tb^{3+}–O) in the glassy structure of Tb^{3+}–$Li_2B_4O_7$ dominate in the second group (<200 cm^{-1}). Note that terbium atoms are much heavier than oxygen ones. That is why the motion of oxygen atoms plays a dominant role in the vibrational stretching modes of Tb–O bonds.

Note also that normal vibrations of the [LiO_6] frameworks also contribute to a frequency interval of 70–450 cm^{-1} [17, 18, 23, 25, 26, 28–32, 42, 43]. Therefore, in this interval, the shifts of the maximum positions in the Raman spectra of the $Li_2B_4O_7$–Tb_2O_3 system with respect to the normal frequencies of internal vibrations of Tb^{3+}–O–Tb^{3+} or O–Tb^{3+}–O are possible due to distortions of the octahedral clusters [Tb_2O_7] and the octahedral complexes [TbO_7].

In the considered frequency interval (70–600 cm^{-1}), mixed translational (at 441 and 488 cm^{-1}) and vibrational (at 538 cm^{-1}) oscillations of lithium ions also appear [27], as well as vibrational oscillations of oxygen atoms (at 246 cm^{-1}) [42]. In this case, the intensities of the bands with the maxima at the frequencies 441 and 538 cm^{-1} are much higher than in the case of stoichiometric composition (Fig. 2, *a*). In our opinion, this is a result of changes in the length of chemical bonds and the angles between them in the LTB matrix owing to the inclusion of octahedral structural units of the Tb_2O_3 oxide.

The frequency interval of 70–600 cm^{-1} also includes the frequencies of "external" vibrations of the structural complexes included in the matrix of glassy LTB, vibrational oscillations of [LiO_6] frameworks, and vibrational oscillations of groups [BO_3] and [BO_4] in the structure of the $[B_4O_7]^{2-}$ cluster as a whole [19, 31, 42]. However, the contribution of those vibrations to the revealed structure of the Raman spectra of activated LTB is insignificant.

Let us now consider the structure of Raman spectra that is observed at frequencies above 600 cm^{-1}. According to the available data [9,14,15,19,20,29,31–33] and taking into account the deformation of the glassy $Li_2B_4O_7$ matrix, the observed maxima can be explained as a result of vibrations related to symmetric deformation (at 768 cm^{-1}), symmetric stretching (at 956 cm^{-1}) of [BO_3] groups, and deformation of [BO_4] groups (at 1024, 1093, and 1121 cm^{-1}). The broad structural diffuse band with maxima at the frequencies 1293, 1350, and 1436 cm^{-1} arises due to the superposition of vibrational oscillations of borate rings (at 1350 cm^{-1}), symmetric stretching of [BO_3] groups (at 1436 cm^{-1}), and vibrations of [TbO_6] structural complexes (at 1293 cm^{-1}). In addition, a certain contribution to the intensity of the maximum at the frequency 1293 cm^{-1} is also given by the normal vibrations of boron-oxygen (B–O) bonds. Note that the activation of glassy LTB with terbium oxide leads to an increase in the frequencies of symmetric deformation (from 763 to 768 cm^{-1}) and symmetric stretching (from 1428 to 1436 cm^{-1}) of the [BO_3] group.

Vibrations of octahedral structural complexes [TbO_6] are also responsible for the appearance of maxima at the frequencies 1605 and 1653 cm^{-1} (Fig. 2, *e*). As concerning the broad diffuse band with a maximum at 1891 cm^{-1}, in our opinion, it arises due to the superposition of linear vibrations of the Tb^{3+}–O–Tb^{3+} or O–Tb^{3+}–O chains in the structure of octahedral [Tb_4O_7], [Tb_2O_3], and [TbO_2] clusters, as well as B–O–B chains in structural [B_4O_7] complexes [13–15].

Unfortunately, the currently available data [9, 13–15, 18–20, 28, 29, 31–34, 39] are insufficient to unambiguously explain the nature of the strongly pronounced maximum at the frequency 70 cm^{-1}, which appears in the Raman spectrum at the maximum activator concentration of 0.05 wt% [Fig. 2, *f*], as well as the nature of the weakly intensive maxima at the frequencies 838 and 1232 cm^{-1}.

4. Conclusions

Raman scattering spectra of glassy lithium tetraborate activated with erbium and terbium oxides to various concentrations (0.0005–0.05 wt%) have been studied. It is shown that the introduction of the Er_2O_3 and Tb_2O_3 impurities into the LTB matrix leads to a substantial complication of Raman spectra even at the minimum impurity concentrations. In this case, the structure of the Raman spectra for glassy $Li_2B_4O_7 : Tb_2O_3$ does not practically change if the impurity concentration increases. At the same time, a qualitative change in the structure of Raman spectra is observed for $Li_2B_4O_7 : Er_2O_3$ at high impurity concentrations (0.01–0.05 wt%).

The identification of the obtained Raman spectra is carried out. It is found that most vibrational modes of $Li_2B_4O_7 : Er_2O_3$ and $Li_2B_4O_7 : Tb_2O_3$ glasses are induced by mixed vibrations of various types. In the framework of the medium order approximation, those vibrations are connected with one another by means of a deformed framework structure consisting of boron-oxygen and erbium/terbium-oxygen complexes.

The obtained results testify to the hybridization of the orbits of tricharged Er^{3+} and Tb^{3+} ions in the $Li_2B_4O_7$ matrix. As a result, as the concentration of

the Er_2O_3 and Tb_2O_3 impurities increases, the structure of glassy LTB becomes clustered with the formation of crystallites in the Er/Tb–B_4O_7 system, which gives rise to a partial inclusion of the cubic symmetry of Er_2O_3 and Tb_2O_3 into the tetragonal symmetry of $Li_2B_4O_7$.

The changes revealed in the Raman spectra of glassy LTB activated with erbium and terbium oxides can provide information on the spectroscopic manifestation of impurity scattering, and they can be used to determine the crystallographic parameters of borates of various types.

1. I. Kindrat, B. Padlyak, R. Lisiecki, V. Adamiv. Spectroscopic and luminescent properties of the lithium tetraborate glass co-doped with Nd and Ag. *J. Alloy. Compd.* **853**, 157321 (2021).
2. I. Kindrat, B. Padlyak, R. Lisiecki, V. Adamiv. Spectroscopic and luminescent properties of the lithium tetraborate glass co-doped with Tm and Ag. *J. Luminesc.* **25**, 117357 (2020).
3. I. Kindrat, B. Padlyak, B. Kuklinski, A. Drzewiecki, V.T. Adamiv. Effect of silver co-doping on enhancement of the Sm^{3+} luminescence in lithium tetraborate glass. *J. Luminesc.* **213**, 290 (2019).
4. I. Kindrat, B. Padlyak, R. Lisiecki, A. Drzewiecki, V.T. Adamiv. Effect of silver co-doping on luminescence of the Pr^{3+}-doped lithium tetraborate glass. *J. Luminesc.* **241**, 118468 (2022).
5. M.A. Vallejo, S. Romero-Servin, M. Alvarez, J. Angel, C. Gomez-Solis, L. Alvarez-Valtierra, M.A. Sosa. Enhancing the nonlinear optical properties of lithium tetraborate glass using rare earth elements and silver nanoparticles. *Nano* **5**, 2050064 (2020).
6. J. Krogh-Moe. Refinement of the crystal structure of lithium diborate Li_2O–$2B_2O_3$. *Acta Cryst. B* **24**, 1791 (1968).
7. A. Senyshyn, B. Schwarz, T. Lorenz, V.T. Adamiv, Ya.V. Burak, J. Banys, R. Grigalaitis, L. Vasylechko, H. Ehrenberg, H. Fuess. Low-temperature crystal structure, specific heat, and dielectric properties of lithium tetraborate $Li_2B_4O_7$. *J. Appl. Phys.* **108**, 093524 (2010).
8. A.K. Yadav, P. Singh. A review of the structures of oxide glasses by Raman spectroscopy. *RSC Adv.* **5**, 67583 (2015).
9. L. Chervinka. Medium-range order in amorphous materials. *J. Non-Cryst. Sol.* **106**, 291 (1988).
10. K. Nakamoto. *Infrared and Raman Spectra of Inorganic and Coordination Compounds* (John Wiley and Sons, 1991) [ISBN: 978-0-471-74493-2].
11. J. Lorösch, M. Couzi, J. Pelous, R. Vacher, A. Levasseur. Brillouin and Raman scattering study of borate glasses. *J. Non-Cryst. Sol.* **69**, 1 (1984).
12. R. Shuker, R.W. Gammon. Raman-scattering selection-rule breaking and the density of states in amorphous materials. *Phys. Rev. Lett.* **25**, 2225 (1970).
13. N. Imanaka, T. Masui, W.Y. Kim. First electrochemical growth of $Tb_{16}O_{30}$ single crystal. *J. Sol. St. Chem.* **177**, 38392 (2004).
14. J. Cui, G.A. Hope. Raman and fluorescence spectroscopy of CeO_2, Er_2O_3, Nd_2O_3, Tm_2O_3, Yb_2O_3, La_2O_3, and Tb_4O_7. *J. Spectrosc.* **2015**, 8 (2015).
15. J. Ibanez, O. Blazquez, S. Hernandez, B. Garrido, P. Rodriguez-Hernandez, A. Munoz, M. Velazquez, P. Veber, F.J. Manjon. Lattice dynamics study of cubic Tb_2O_3. *J. Raman Spectrosc.* **49** (12), 2021 (2018).
16. P.S. Danilyuk, P.P. Puga, A.I. Gomonai, V.N. Krasylynec, P.N. Volovich, V.M. Rizak. X-ray luminescence and spectroscopic characteristics of Er^{3+} ions in a glassy lithium tetraborate matrix. *Opt. Spectrosc.* **118**, 924 (2015).
17. T. Lopez, E. Haro-Poniatowski, P. Bosh, M. Asomoza, R. Gomez, M. Massot, M. Balkanski. Spectroscopic characterization of lithium doped borate glasses. *J. Sol-Gel Sci. Technol.* **2**, 8914 (1994).
18. Y. Li, G. Lan. Pressure-induced amorphization study of lithium diborate. *J. Phys. Chem. Solids* **57**, 887 (1996).
19. Yu.K. Voronko, A.A. Sobol, V.E. Shukshin. Raman spectroscopy study of the phase transformations of LiB_3O_5 and $Li_2B_4O_7$ during heating and melting. *Inorg. Mater.* **49**, 923 (2013).
20. F.H. El Batal, A.A. El Kheshen, M.A. Azooz, S.M. Abo-Naf. Gamma ray interaction with lithium diborate glasses containing transition metals ions. *Opt. Mater.* **30**, 881 (2008).
21. M. Massot, E. Haro, M. Oueslati, M. Balkanski, A. Levasseur, M. Menetrier. Structural investigation of doped lithium borate glasses. *Mater. Sci. Eng. B* **3**, 57 (1989).
22. P.P. Puga, P.S. Danyliuk, G.V. Rizak, A.I. Gomonai, I.M. Rizak, V.M. Rizak, G.D. Puga, L. Kvetkova, M.M. Byrov, I.I. Chychura, V.N. Zhiharev. Raman scattering in glassy $Li_2B_4O_7$. *J. Chem. Techn.* **26**, 30 (2018).
23. V.T. Adamiv, T. Berko, A.V. Kityk, Ya.V. Burak, V.I. Dzhala, V.I. Dovgij, I.E. Moroz. On the phonon spectra of borate single crystals. *Ukr. J. Phys.* **37**, 368 (1992).
24. T.D. Kelly, J.C. Petrosky, J.W. McClory, V.T. Adamiv, Ya.V. Burak, B.V. Padlyak, I.M. Teslyuk, N. Lu, L. Wang, W-N. Mei, P.A. Dowben. Rare earth dopant (Nd, Gd, Dy, and Er) hybridization in lithium tetraborate. *Front. Phys. Ser. Condens. Matter Phys.* **2**, No. 31, 1 (2014).
25. G.L. Paul, W. Taylor. Raman spectrum of $Li_2B_4O_7$. *J. Phys. C* **15**, 1753 (1982).
26. S. Furusawa, S. Tange, Y. Ishibashi, K. Miwa. Raman scattering study of lithium diborate ($Li_2B_4O_7$) single crystal. *J. Phys. Soc. Japan* **59**, 825 (1990).
27. Ya.V. Burak, V.I. Dovgij, A.V. Kityk. Longitudinal-transverse splitting of phonon modes in the $Li_2B_4O_7$ crystals. *J. Appl. Spectrosc.* **52**, 126 (1990).

28. T. Berko, V.I. Dovgij, A.V. Kityk, Ya.V. Burak, V.I. Dzhala, I.E. Moroz. Raman spectra of lithium tetraborate monocrystals. *Ukr. J. Phys.* **38**, 39 (1993).
29. Q. Hu, T. Wang, Y. Chu, X. Wang, Y. Du, J. Ren, X. Yang, G. Yang, X. Kong, P. Wang. Mixed alkali effects in Er^{3+}-doped borate glasses: Influence on physical, mechanical, and photoluminescence properties. *J. Am. Ceram. Soc.* **102**, 4562 (2019).
30. G. Chandrashekaraiah, A. Jayasheelan, M. Gowri, N.S. Reddy, C.N. Reddy. Correlation between non-linear optical parameter and structure of $Li_2B_4O_7$ glasses doped with Er^{3+} ions. *J. Non-Cryst. Solids* **531**, 119843 (2020).
31. A.E. Elalaoui, A. Maillard, M.D. Fontana. Raman scattering and non-linear optical properties in $Li_2B_4O_7$. *J. Phys.: Cond. Matter* **17**, 7441 (2005).
32. A.V. Vdovin, V.N. Moiseenko, V.S. Gorelik, Ya. Burak. Vibrational spectrum of $Li_2B_4O_7$ crystals. *Phys. Solid State* **43**, 1648 (2001).
33. V.N. Moiseenko, A.V. Vdovin, Ya. Burak. Efficiency of the Raman scattering in the $Li_2B_4O_7$ crystals. *Opt. Spectrosc.* **81**(4), 620 (1996).
34. N.T. McDevitt, A.D. Davidson. Infrared lattice spectra of cubic rare earth oxides in the region 700 to 50 cm^{-1}. *J. Opt. Soc. Am.* **56**, 636 (1966).
35. G. Schaack, J.A. Koningstein. Phonon and electronic Raman spectra of cubic rare-earth oxides and isomorphous yttrium oxide. *J. Opt. Soc. Am.* **60**, 1110 (1970).
36. R. Tomar, P. Kumar, A. Kumar, A. Kumar, P. Kumar, R.P. Pant, K. Asokan. Investigations on structural and magnetic properties of Mn doped $Er_{(2)}O_{(3)}$. *Solid State Sciences* **67**, 8 (2017).
37. A.M. Lejus, D. Michel. Raman spectrum of $Er_{(2)}O_{(3)}$ sesquioxide. *Physica Status Solidi B* **84**, K105 (1977).
38. L.A. Tucker, F.J. Carney, P. McMillan, S.H. Lin, L. Eyring. Raman and resonance Raman spectroscopy of selected rare-earth sesquioxides. *Appl. Spectrosc.* **38**, 857 (1984).
39. D. Yan, P. Wu, S.P. Zhang, L. Liang, F. Yang, Y.L. Pei, S. Chen. Assignments of the Raman modes of monoclinic erbium oxide. *J. Appl. Phys.* **114**, 193502 (2013).
40. A.N. Lazarev, A.P. Mirgorodsky, I.S. Ignatiev. *Vibrational Spectra of Complex Oxides. Silicates and Their Analogues.* (Nauka, 1975) (in Russian).
41. M.V. Abrashev, N.D. Todorov, J. Geshev. Raman spectra of $R_{(2)}O_{(3)}$ (R – rare earth) sesquioxides with C-type bixbyite crystal structure: A comparative study. *J. Appl. Phys.* **116**, 103508 (2014).
42. Ya.V. Burak, V.T. Adamiv, I.M. Teslyuk. To the origin of vibrational modes in Raman spectra of $Li_2B_4O_7$ single crystals. *Func. Mater.* **13**, 591 (2006).
43. Ya.V. Burak, I.B. Trach, V.T. Adamiv, I.M. Teslyuk. Isotope effect in the Raman spectra of $Li_2B_4O_7$ single crystals. *Ukr. J. Phys.* **47** 923 (2002).

Received 05.04.24.
Translated from Ukrainian by O.I. Voitenko

П.С. Данилюк, Г.В. Різак, О.І. Гомонай,
П.П. Пуга, А.О. Фролов, Г.М. Гомонай, В.М. Різак

КОМБІНАЦІЙНЕ РОЗСІЮВАННЯ СВІТЛА СКЛОПОДІБНИМ ТЕТРАБОРАТОМ ЛІТІЮ, АКТИВОВАНИМ ОКСИДАМИ ЕРБІЮ ТА ТЕРБІЮ

Досліджено спектри комбінаційного розсіювання склоподібного тетраборату літію, активованого оксидами ербію та тербію різної концентрації. Встановлено, що основну частину структури спектрів комбінаційного розсіювання досліджених зразків скла $Li_2B_4O_7 : Er_2O_3$ та $Li_2B_4O_7 : Tb_2O_3$ у межах усередненого порядку зумовлено змішаними коливаннями складних бор/літій/ербій/тербій-кисневих структурних комплексів.

Ключові слова: комбінаційне розсіювання, тетраборат літію, оксид ербію, оксид тербію, структурні комплекси, змішані коливання, фонони.